Advances in Materials Research, *Vol. 15, No. 1 (2026) 69-82*
https://doi.org/10.12989/amr.2026.15.1.069

Techno-Press

Effect of heat treatments on microstructure and properties of TiNiCu shape memory alloys developed through powder metallurgy

Abid Hussain*[1], Afzal Khan[1], Muhammad Imran Khan[2], Saif Ur Rehman[3], Asnaf Aziz[1]

[1]*Department of Mechanical Engineering, University of Engineering and Technology, Peshawar, Pakistan, 25100*
[2]*Faculty of Materials and Chemical Engineering, Ghulam Ishaq Khan (GIK) Institute of Science, Engineering and Technology, Khyber Pakhtonkhwa, Pakistan*
[3]*Institute of Industrial Control System, Rawalpindi, Pakistan*

(Receive September 27, 2024, Revised January 22, 2026, Accepted February 23, 2026)

Abstract. This research paper explores the development and characterization of three Ti-Ni-Cu shape memory alloys (SMAs), $Ti_{50}Ni_{40}Cu_{10}$, $Ti_{50}Ni_{38}Cu_{12}$, and $Ti_{50}Ni_{35}Cu_{15}$, synthesized through powder metallurgy. We investigate the effects of various heat treatments, including solution treatment, annealing, and aging, on their microstructure and properties. Comprehensive analyses, including Differential Scanning Calorimetry (DSC), Scanning Electron Microscopy (SEM), Energy-Dispersive X-ray spectroscopy (EDX), and percentage porosity measurements, were conducted. This study aims to study the influence of heat treatment processes on SEM morphology, EDX, DSC thermal transitions, porosity, and density of the SMAs. From the DSC results, it is evident that transformation temperatures increase with higher Cu content in the solution-treated, annealed, and aged samples. The percentage porosity and pore size increase with higher Cu content in all heat treatment processes, but the minimum percentage porosity and smallest pore sizes are observed in the annealed samples. SEM images confirm the presence of porosity and reveal the pore sizes. Optical microscopy shows that grain size increases with higher Cu content.

Keywords: advanced materials; aging; annealing; porosity; scan electronic microscopy

1. Introduction

(Bogue 2009) have demonstrated that shape memory alloys (SMAs) are advanced materials that exhibit the unique ability to return to a predetermined shape upon heating [1]. According to (Parvizi et al. 2021), Ti-Ni-Cu systems have garnered significant interest due to their potential applications in actuators, medical devices, and aerospace components [2]. As described by (Ahmad et al. 2024) the mechanical properties and functional performance of these SMAs are profoundly influenced by their microstructure, which can be controlled through heat treatments during the powder metallurgy processing route [3]. (Singh et al. 2021) studied that powder metallurgy is a cost-effective method for producing SMAs, enabling precise control over alloy composition and microstructure [4]. This study aims to evaluate the effects of various heat treatments

*Corresponding author, Ph.D., Assistant Professor, E-mail: abidhussain@uetpeshwar.edu.pk

ISSN: 2234-0912 (Print), 2234-179X (Online)

on the microstructural evolution and properties of Ti-Ni-Cu alloys produced via this route.

(Aghamiri et al. 2013) studied that TiNiCu SMAs, a subset of the broader Ti-Ni family, incorporate copper into the traditional titanium-nickel (Ti-Ni) alloy system. The addition of copper modifies the phase transformation characteristics and mechanical properties of the SMAs. TiNiCu SMAs exhibit a range of desirable properties, including high strength, excellent fatigue resistance, and a broad range of transformation temperatures [5]. (Shiva et al. 2016) described the characteristics make them particularly suitable for applications in fields such as aerospace, automotive engineering, biomedical devices, and robotics. The phase transformation in TiNiCu alloys involves a reversible change between the austenite phase, which is stable at higher temperatures and has a cubic crystalline structure, and the martensite phase, which is stable at lower temperatures and often adopts a more complex orthorhombic or monoclinic structure [6]. (Tong et al. 2020) described that transformation is accompanied by significant changes in mechanical properties, such as stiffness and ductility. The temperature at which these transformations occur, known as the transformation temperatures, is crucial for determining the practical utility of the SMAs in specific applications. Thermomechanical treatment is a critical process for tailoring the properties of TiNiCu SMAs [7]. (Radhamani and Balakrishnan 2023) and aging (Li 2017) studied that treatment involves a sequence of thermal and mechanical operations, including solution treatment, annealing. Solution treatment, typically performed at high temperatures, homogenizes the alloy and dissolves any secondary phases or precipitates. Rapid quenching that follows transforms the alloy into a metastable state, annealing involves the heating of an SMAs to a specific temperature and then cold rolled up to 40%, while aging at intermediate temperatures can precipitate fine particles that strengthen the material and refine its microstructure [8, 9]. (Shiva et al. 2019) presented that treatments impact several aspects of the TiNiCu SMAs performance [10].

(Lu et al. 2022) and (Zaefferer et al. 2004) described that the thermal history and mechanical processing affect the size, distribution, and morphology of precipitates and grains within the SMA. These microstructural changes play a pivotal role in determining the transformation temperatures and the overall mechanical behavior of the SMA. The phase transformation temperatures and the hysteresis between the austenite and martensite phases can be significantly influenced by thermomechanical treatments [11, 12]. (Karimzadeh et al. 2015) studied that these changes affect the material's responsiveness to temperature changes and its ability to recover its original shape after deformation. The strength, ductility, and fatigue resistance of TiNiCu SMAs are closely linked to the thermomechanical treatment processes [13]. (Panton 2016) properly optimized treatments can enhance the material's performance by improving its yield strength, elongation, and cyclic stability [14].

According to (Aghamiri et al. 2013) DSC was employed to investigate the reversible martensitic phase transformation peaks of the alloy, which are indicative of its shape memory effect (SME). The analysis of these endothermic and exothermic peaks utilized the tangent differentiation method, executed automatically by the DSC software on a manually selected segment of the DSC curve [5]. This approach allowed for the determination of the key thermodynamic parameters of the SMA, including the characteristic martensitic transformation temperatures identified as working temperatures, below 100 ℃, as well as the associated enthalpy changes.

This research paper aims to systematically investigate the effects of various thermomechanical treatments on the properties of TiNiCu SMAs. By examining different heat treatment processes such as solution treatment, annealing and aging, we seek to understand how these factors influence the microstructural, transformation temperatures, porosity and thermal hysteresis of the SMA. The

Table 1. Average particle size and purity of elemental powder

Elemental Powder	Titanium	Nickel	Copper
Model	99.29	99.29	99.29
A-GGBS	34.99	1.98	2.48

study will provide a comprehensive analysis of the relationship between treatment parameters and SMA performance, contributing valuable insights into the optimization of TiNiCu SMAs for specific applications. The findings from this research will offer a deeper understanding of the processing-property relationships in TiNiCu SMAs, aiding in the design and development of advanced materials with tailored properties for diverse engineering applications. This study will also lay the groundwork for future research aimed at further enhancing the performance and functionality of TiNiCu SMAs.

2. Materials and methods

The SMAs were prepared through powder metallurgy route using titanium (Ti), nickel (Ni) and copper (Cu) powders. The particle size of Ti, Ni and Cu were measured with the help of Imaj J software. The particle size and purity of elemental powders are shown in Table 1. Accurately weigh the required amount of Ti, Ni and Cu powders using weight balance as shown in Figure 1a. Use Probe Sonicator to uniformly mix the elemental powders as shown in Fig. 1b. The powders of Ti, Ni and Cu were mixed with ethanol to form a slurry. The slurry is placed in a container, and an ultrasonic probe is immersed in the container. The probe is connected to an ultrasonic generator that produces high-frequency sound waves. The ultrasonic generator emits high-frequency sound waves, which are transmitted through the probe into the slurry. These sound waves create rapid pressure changes and shear forces in the liquid. The pressure changes cause the formation and collapse of microscopic bubbles in the liquid a process known as cavitation. This generates intense local energy, which breaks up clumps and spreads the powders more evenly. The energy from the cavitation effectively breaks down clumps of powder and improves the homogeneity of the mixture. It helps in achieving a uniform distribution of particles throughout the liquid. A hot plate was used to dry a wet mixture after sonication. It is a common and effective method for removing excess liquid and concentrating the mixture as shown in Fig. 1c. The mixed powders were transferred into a hydraulic press to form pellets as shown in Fig. 1d. A uniaxial pressure of 800 MPa were applied to achieve a pellet density suitable for sintering. The compacted pellets were placed in a high-temperature Vacuum furnace. Ensure that the furnace is clean and preheated to the desired temperature of 950 °C for 1 hour. Three samples were prepared $Ti_{50}Ni_{40}Cu_{10}$, $Ti_{50}Ni_{38}Cu_{12}$ and $Ti_{50}Ni_{35}Cu_{15}$. The SMAs were names as Cu_{10}, Cu_{12} and Cu_{15} according to the atomic percentage of Cu.

After evacuation, each sample was enclosed in individual quartz tubes and purged with pure argon gas to initiate the solution treatment process. Subsequently, the SMAs were introduced into a vacuum furnace preheated to 900 °C and held at this temperature for a duration of two hours, ensuring a consistent temperature of 900 °C throughout. Upon completion of the procedure, the samples were swiftly cooled within the quartz tubes. To mitigate the risk of tube fracture, the rapid cooling process was conducted using cold water. After the solution treatment, the SMAs

(a) Weight balance

(b) Sonicator

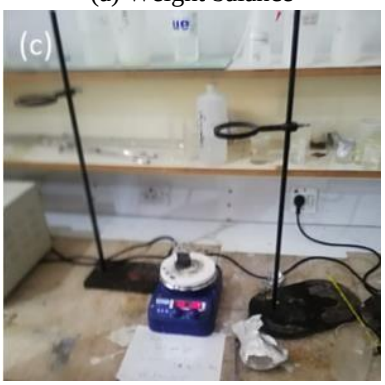

(c) Hot plate

(d) Compactor

Figure 1. Experimental Procedures for preparation of TiNiCu SMAs

undergoes annealing at 950 ℃ to assess their properties under these conditions and cold rolled upto 40%. The remaining solution treated SMAs were aged at 950 ℃. Samples from alloys 10Cu, 12Cu, and 15Cu followed the same encapsulation process in quartz tubes as the solution-treated samples. These sealed tubes were then positioned in a tube furnace preheated to an aging temperature of 950 ℃. Subsequently, the three SMAs were aged for a duration of four hours at this temperature. Before undergoing SEM analysis, the materials underwent mechanical grinding. Subsequently, they were polished using a refined technique involving an alumina slurry containing particles as small as 0.5 microns. Prior to SEM examination, thorough preparation of the materials was conducted. DSC is a commonly used method for precisely evaluating the thermal characteristics of specimens. It utilizes a differential technique to directly gauge the heat exchanged by SMAs during processes like heating, cooling, or maintaining a constant temperature. DSC allows for the exploration of various thermal phenomena taking place within the SMAs by measuring the energy required to sustain a particular temperature. Phase transitions within the SMAs are evident as sudden shifts in release or absorption of heat during heating or cooling stages. These transitions appear as distinct peaks on the DSC graph, offering valuable understanding into the changes happening within the SMAs.

The 900 ℃, 2 hours solution treatment was primarily selected in order to promote chemical homogenization as well as dissolve non-equilibrium phases that occur during solidification or prior to thermo-mechanical transformation. Temperatures close to 900 ℃ are used in TiNiCu SMAs to

eliminate compositional segregation, and to dissolve Cu rich secondary phases and form a chemically homogeneous B2 austenitic matrix. Simultaneously, this temperature is not sufficiently high to reach excessive temperatures of grain growth or incipient melting which might happen at warmer temperatures. This treatment is therefore only a kind of homogenization step and not a classical solution treatment as is the case with precipitation-hardening alloys.

The annealing treatment that followed was purposefully done at a high temperature of 950 ℃, in order to enhance thermodynamic equilibrium and stabilization of the phases. At this temperature, an improvement in the atomic diffusion results in a full stabilization of B2 parent phase, reduction of residual stresses, and the adjustment of phase fraction by suppressing metastable phases. In TiNiCu alloys, more annealing is usually needed to obtain consistent and reliable martensitic transformation behavior, especially with the addition of Cu to be able to adjust the transformation temperatures and to minimize the width of hysteresis.

The heat treatment at 950 ℃ is, however, not equivalent to the traditional low-temperature precipitation aging, despite the name aging. Rather, this exposure at high temperature, in TiNiCu case, is aimed at equilibrium phase formation, stabilization of Cu-substituted TiNi phases, and improvement of the thermal and functional stability of martensitic transformations. TiNiCu alloys do not rely on the formation of fine precipitates to strengthen the alloy as is done to classical precipitation-strengthened alloys. Instead, they are dictated by phase stability, chemical homogeneity as well as a transformation thermodynamics which frequently involves high-temperature equilibration treatments.

The porosity (%) of nine samples was measured on the basis of density according to (Purohit et al.) Eq. (1) [15].

$$\%\, Porosity = 1 - \frac{P_r}{P_0} \times 100 \tag{1}$$

where P_r represent the real density of the SMAs and P_0 represent the theoretical density of the SMA. Real density of the SMA can be determined by dividing mass by volume and theoretical density can be determined by using Eq. 2 [15].

$$P_0 = \left[\left(P_0^{Ni} \times at.\%Ni\right)\right] + \left[\left(P_0^{Cu} \times at.\%Cu\right)\right] + \left[\left(P_0^{Ti} \times at.\%Ti\right)\right] \tag{2}$$

where $p_o{}^{Ni}$, $p_o{}^{Cu}$ and $p_o{}^{Ti}$ represents the theoretical densities of Ni, Cu and Ti.

3. Results and discussions

3.1 DSC Analysis

Tables DSC measurements were conducted to find the transformation temperatures of the Ti–Ni–Cu SMAs. The experiments were performed under a controlled atmosphere at a constant heating and cooling rate of 10 ℃/min over the selected temperature range. DSC results revealed distinct thermal transitions corresponding to the phase transformations in the Ti-Ni-Cu SMAs. The solution-treated samples generally exhibited a higher transformation temperature compared to annealed and aged samples. This can be attributed to the dissolution of secondary phases and enhanced solid solution strengthening during solution treatment. In Solution treatment the transformation temperature increases as shown in Fig. 2. The transformation temperatures

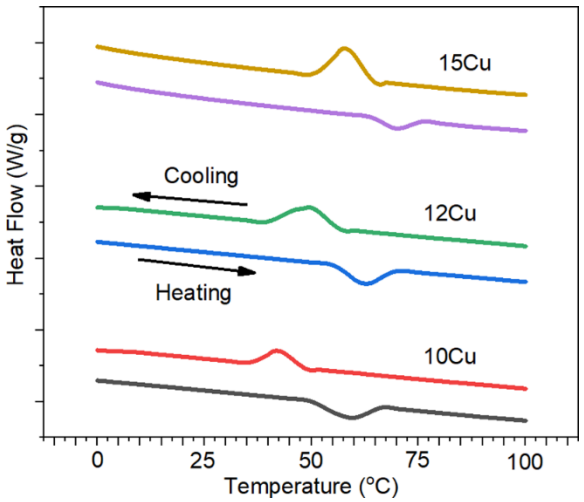

Figure 2. Solution Treatment of Cu_{10}, Cu_{12} and Cu_{15} SMAs

Table 2. Transformation temperatures for 10Cu, 12Cu and 15Cu solution treated SMAs

SMAs	Transformation Temperature (°C)				Thermal Hysteresis
	Ms	M_f	A_s	A_f	A_f - M_s
$Ti_{50}Ni_{40}Cu_{10}$	45	37	49	69	24
$Ti_{50}Ni_{38}Cu_{12}$	48	39	51	73	25
$Ti_{50}Ni_{35}Cu_{15}$	52	42	55	76	22

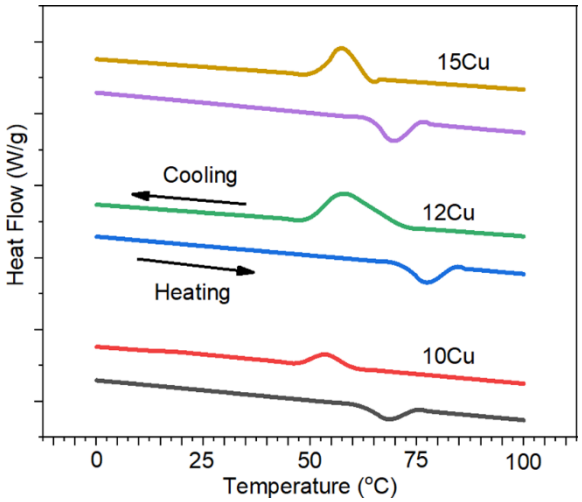

Figure 3. Annealing of Cu_{10}, Cu_{12} and Cu_{15} SMAs

Martensite Start Temperature (Ms), Martensite Final Temperature Mf), Austenite Temperature (A_s), and Austenite Final Temperature (A_f) are determined from Fig. 2 by linear intercept method and are presented in Table 2. It is clear from Fig. 2 that in solution treatment for all SMAs the transformation temperature increases while negligible change in thermal hysteresis. It is clear from

Table 3. Transformation temperatures for 10Cu, 12Cu and 15Cu annealed SMAs

SMAs	Transformation Temperature (°C)				Thermal Hysteresis
	M_s	M_f	A_s	A_f	A_f - M_s
$Ti_{50}Ni_{40}Cu_{10}$	55	49	63	79	24
$Ti_{50}Ni_{38}Cu_{12}$	58	51	61	81	23
$Ti_{50}Ni_{35}Cu_{15}$	62	54	65	85	23

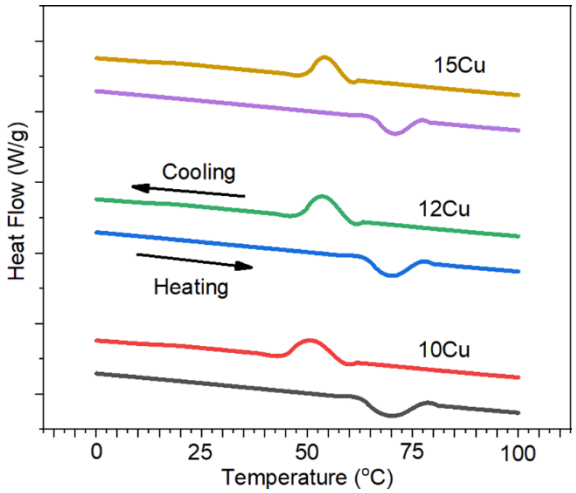

Figure 4. Aging of Cu_{10}, Cu_{12} and Cu_{15} SMAs

Table 4. Transformation temperatures for 10Cu, 12Cu and 15Cu aged SMAs

SMAs	Transformation Temperature (°C)				Thermal Hysteresis
	M_s	M_f	A_s	A_f	A_f - M_s
$Ti_{50}Ni_{40}Cu_{10}$	58	48	62	82	24
$Ti_{50}Ni_{38}Cu_{12}$	61	50	64	85	24
$Ti_{50}Ni_{35}Cu_{15}$	65	52	68	88	23

Fig. 3 that in annealing increases both the martensitic and austenitic transformation temperatures. This is due to the reduction of internal stresses and the improvement of the material's microstructure. The transformation temperature and thermal hysteresis determined from Fig. 3 are shown in Table 3. The values of thermal hysteresis shown in Table 3 are valid for practical applications. In aging both the martensitic and austenitic transformation temperatures increase due to the formation of precipitates or other microstructural changes that affect the phase transformation as shown in Fig. 4. The transformation temperatures and thermal hysteresis are presented in Table 4.

In summary, annealing, aging, and solution treatment each have distinct effects on the DSC profile of SMAs. Annealing generally leads to more uniform and predictable transformations with higher transformation temperatures, aging can increase temperatures and broaden peaks due to microstructural changes, and solution treatment can restore or optimize transformation behavior by altering the phase composition and distribution.

Table 5. Percentage porosity of SMAs

Sample No.	Composition	Heat Treatment	Porosity (%)
1	$Ti_{50}Ni_{40}Cu_{10}$	Solution Treated	17.87
2	$Ti_{50}Ni_{38}Cu_{12}$	Solution Treated	19.65
3	$Ti_{50}Ni_{35}Cu_{15}$	Solution Treated	20.92
4	$Ti_{50}Ni_{40}Cu_{10}$	Annealed	16.32
5	$Ti_{50}Ni_{38}Cu_{12}$	Annealed	18.41
6	$Ti_{50}Ni_{35}Cu_{15}$	Annealed	19.56
7	$Ti_{50}Ni_{40}Cu_{10}$	Aged	18.05
8	$Ti_{50}Ni_{38}Cu_{12}$	Aged	19.32
9	$Ti_{50}Ni_{35}Cu_{15}$	Aged	20.45

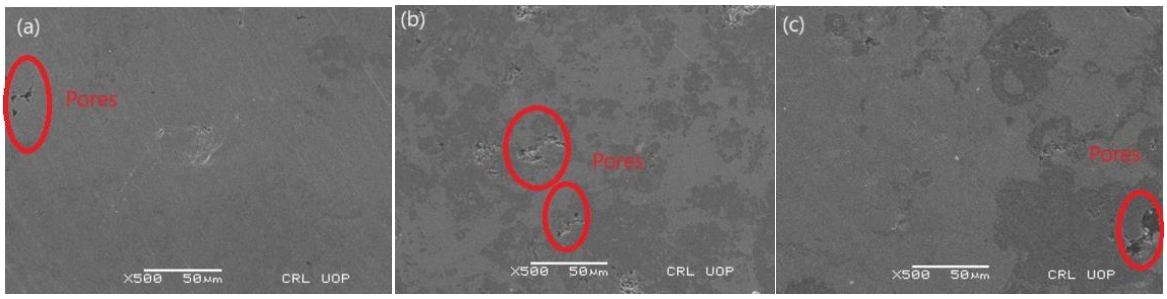

(a) 10Cu SMA (b) 12Cu SMA (c) 15Cu SMA

Figure 5. SEM images of Cu_{10}, Cu_{12} and Cu^{15} Solution Treatment SMAs

3.2 Porosity and density

The Percent porosity was estimated based on the density measurements. The percent porosity of solution treated, annealed and aged SMAs were determined using Eqs. (1, 2) in methods and materials section. From Table 5 it is clear that in solution treatment the percent porosity increases with the increase of Cu contents. Copper addition can affect the solubility of elements and the formation of secondary phases during solution treatment. Generally, the solubility of Cu in the TiNi matrix is limited, leading to the formation of precipitates or secondary phases, such as Ti_2Cu or Ni_4Ti_3. The presence of these secondary phases can potentially increase the tendency for the formation of pores, particularly if the precipitates promote the development of localized stresses or if they are not well-dispersed. From Table 5 it is clear that in annealing the porosity in SMAs increases due to the addition of Cu. During annealing, the role of Cu can influence the stability of precipitates and the coarsening of microstructures. Increased Cu content may lead to more pronounced phase transformations, potentially increasing porosity. In aging the percent porosity increases as shown in Table 5. The addition of Cu increases the percent porosity due to the formation of coarsening precipitates. Fig. 5, SEM images of solution treated SMAs shows that percent porosity and pore size increase with the addition of Cu from Cu10 to Cu15. Because addition of Cu can affect the solubility of elements and the formation of secondary phases during solution treatment. Generally, the solubility of Cu in the TiNi matrix is limited, leading to the formation of precipitates or secondary phases, such as Ti_2Cu or Ni_4Ti_3. The presence of these

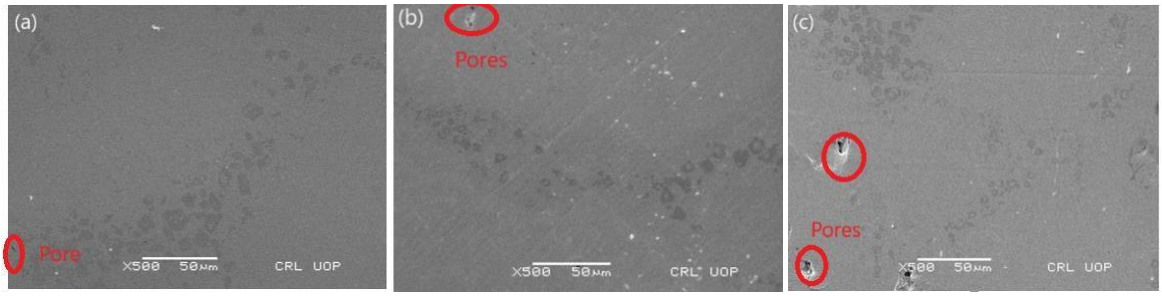

(a) 10Cu SMA (b) 12Cu SMA (c) 15Cu SMA

Figure 6. SEM images of Cu_{10}, Cu_{12} and Cu^{15} annealed SMAs

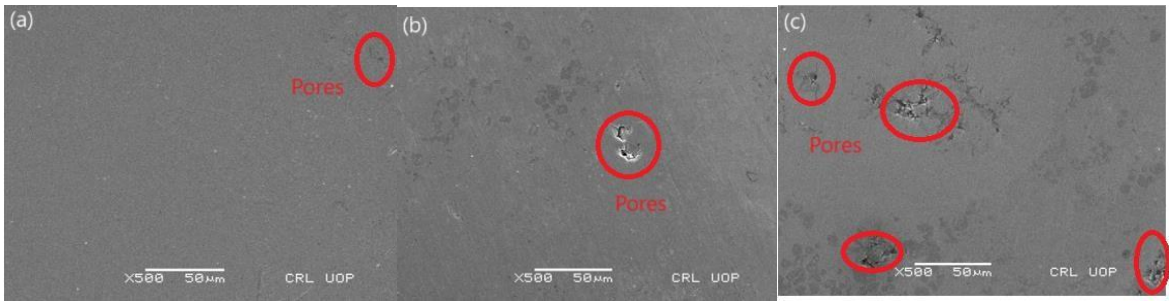

(a) 10Cu SMA (b) 12Cu SMA (c) 15Cu SMA

Figure 7. SEM images of Cu_{10}, Cu_{12} and Cu^{15} aged SMAs

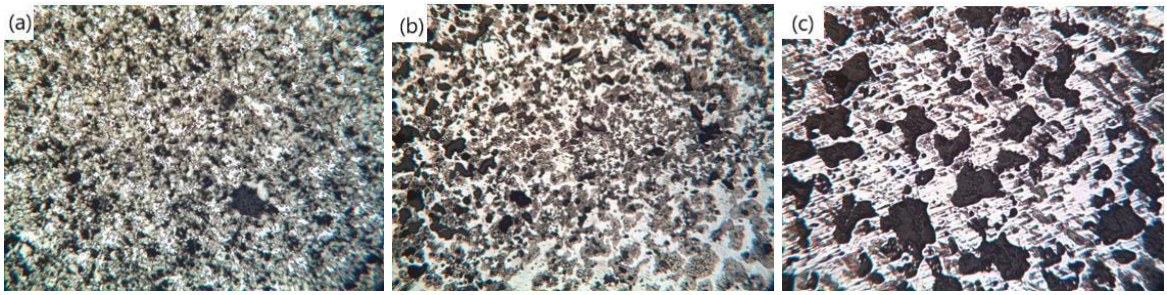

(a) 10Cu SMA (b) 12Cu SMA (c) 15Cu SMA

Figure 8. Optical Microscopy of of Cu_{10}, Cu_{12} and Cu^{15} Solution Treatment SMAs

secondary phases can potentially increase the tendency for the formation of pores, particularly if the precipitates promote the development of localized stresses or if they are not well-dispersed.

Fig. 6 shows the SEM images of annealed SMAs from Cu10 to Cu15. The percent porosity and pore size increase with the increase of Cu contents as shown in Fig. 6. During annealing, the role of Cu can influence the stability of precipitates and the coarsening of microstructures. Increased Cu content may lead to more pronounced phase transformations, potentially increasing porosity if these phases are not well-integrated or if they encourage the formation of voids. Cu addition can also affect the diffusion kinetics, which influences the development of porosity during annealing. The aging treatment increase the percent porosity and pore size due to the formation of large precipitate phases as shown in Fig. 7.

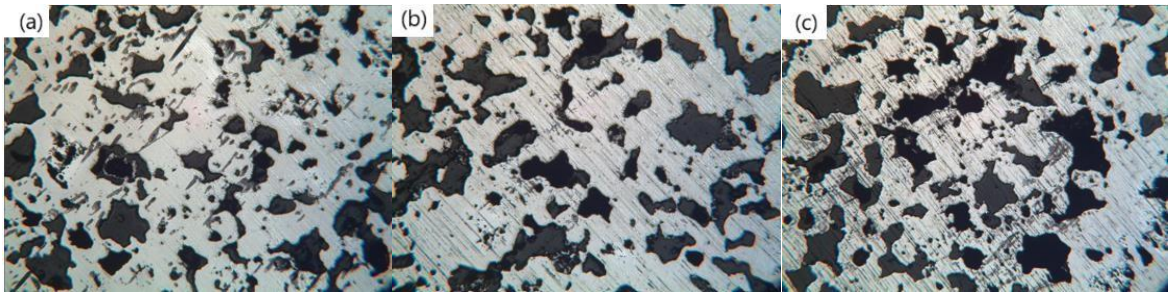

(a) 10Cu SMA (b) 12Cu SMA (c) 15Cu SMA

Figure 9. Optical Microscopy of of Cu_{10}, Cu_{12} and Cu^{15} annealed SMAs

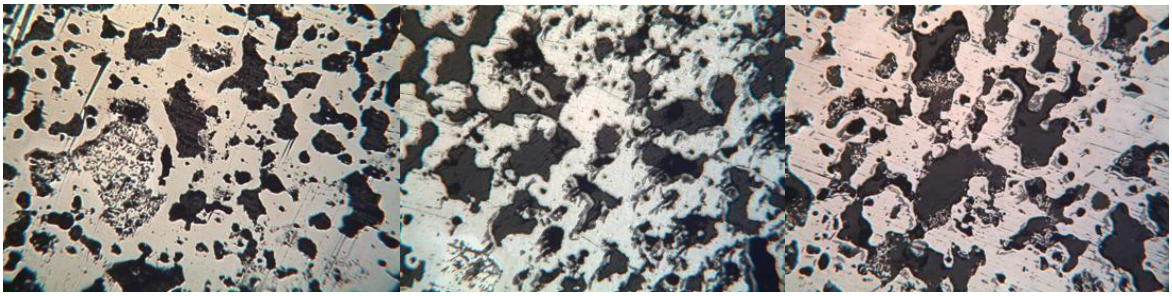

(a) 10Cu SMA (b) 12Cu SMA (c) 15Cu SMA

Figure 10. Optical Microscopy of of Cu_{10}, Cu_{12} and Cu^{15} aged SMAs

Fig. 8 shows the optical microscopy of solution treated SMAs. It is clear from Fig. 8 that with the addition of Cu from Cu10 to Cu15 the grain size could become more heterogeneous or larger due to the need for phase boundary adjustment as Cu promotes the formation of secondary phases

Fig. 9 shows that with the addition of Cu, annealing might lead to more significant grain growth. This is because Cu can influence the phase stability and the migration of grain boundaries, potentially resulting in larger grains.

Fig. 10 shows that with the addition of Cu, Cu promotes the growth of large precipitate phases or affects the matrix in a way that encourages grain coarsening, the grain size might become larger and more uneven.

The combined SEM micrographs and EDX spectra of annealed TiNiCu shape memory alloys with three different Cu content, i.e., Cu_{10}, Cu_{12} and Cu_{15}, are given in Fig. 11 (a-c). The microstructure of the SEM images displays an increasingly changing microstructure as the percentage of Cu increases. The Cu_{10} alloy has a rather dense and uniform microstructure that has small grains and a small number of pores. Conversely, the Cu_{12} and Cu_{15} alloys show an increase in the heterogeneity of the microstructure, as shown by coarser spots and enhanced pore development, which demonstrates the impact of more significant additions in the form of Cu during annealing. The respective EDX spectra indicate the existence of Ti, Ni and Cu in the three compositions. In the case of Cu10 alloy, the Cu peaks are relatively weak and in good balance with the Ti and Ni peaks, indicating that that after the annealing process, Cu is predominantly in the solid solution in the B2 TiNi matrix. As the content of Cu (Cu_{12} and Cu_{15}) increases, the Cu peak intensifies systematically with changes in relative intensities of Ni and Ti peaks. This tendency shows the

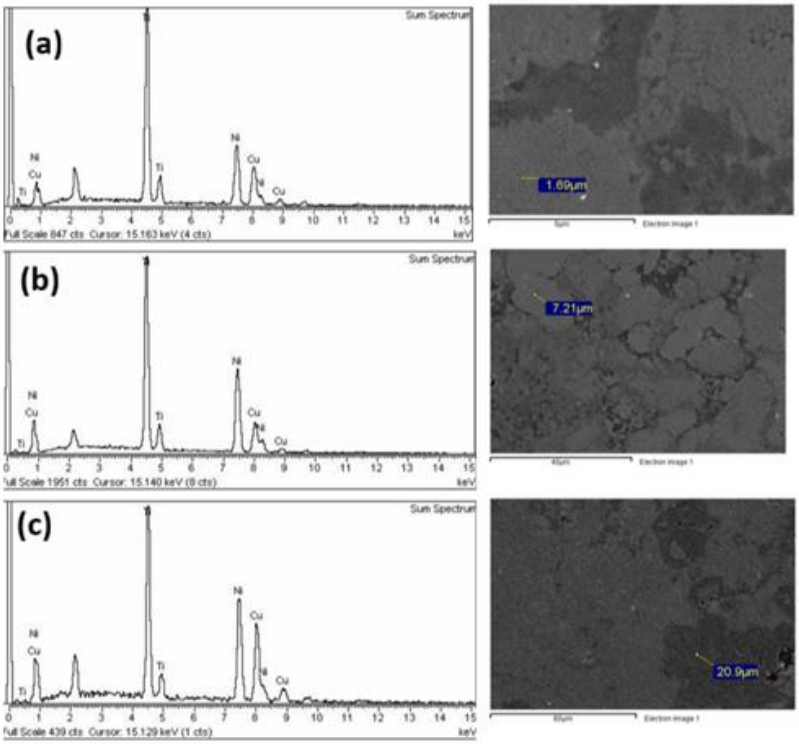

Figure 11. SEM/EDX micrographs of annealed (a) Cu_{10}, (b) Cu_{12} and (c) Cu_{15} SMAs

localized Cu enrichment and compositional inhomogeneity especially in alloy Cu_{15}. The presence of the SEM contrast changes and EDX compositional curves indicates that the solubility limit of Cu in TiNi matrix is surpassed at elevated concentrations of Cu. The atomic diffusion is enhanced during annealing and results in Cu segregation, which presumably results in the development of Cu-rich secondary regions. This phenomenon is well known to occur in TiNiCu shape memory alloys and has generally been linked to the development of secondary intermetallic phases, e.g. Ti_2Cu or Ni_4Ti_3. In spite of the fact that the definite phase identification can be achieved through the XRD analysis, the current SEM-EDX analysis data give a high compositional evidence that the annealed Cu_{12} and Cu_{15} SMAs display segregation of Cu and formation of new phases.

Fig. 12 (a-c) shows the SEM micrographs and EDX spectrum of TiNiCu shape memory alloys containing three different amounts of copper (Cu_{10}, Cu_{12} and Cu_{15}) after an aging process. The aged specimens compared to the annealed one display conspicuous microstructural alterations that can be explained by the prolonged exposure to high temperatures and redistribution of alloying elements due to diffusion. The microstructure of the Cu_{10} alloy is rather homogeneous, with only a little porosity; the corresponding EDX spectrum shows the equal intensity of the Ti, Ni and Cu peaks, which means that the copper is distributed mainly in the TiNi matrix following the aging process. On the other hand, the Cu_{12} and the Cu_{15} alloys show steadily increased surface roughness and the development of larger and more distinct pores or secondary areas, with typical feature sizes of about 16.6 µm for Cu_{12} and as large as 33.8 µm Cu_{15}. These measurements are an indication of augmented diffusion and coarsening as the age progresses. The EDX spectra of the

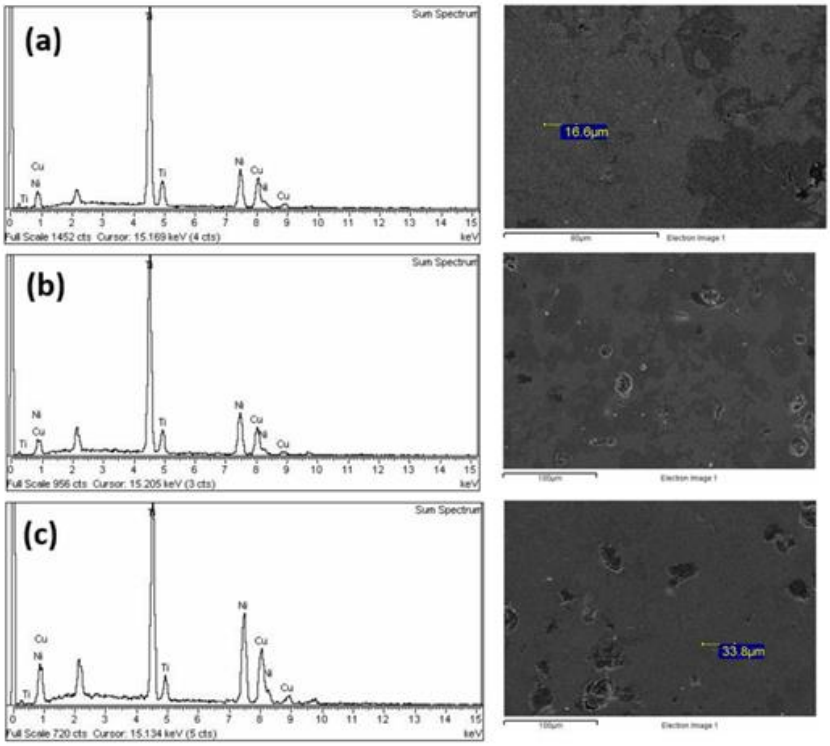

Figure 11. SEM/EDX micrographs of aged (a) Cu_{10}, (b) Cu_{12} and (c) Cu_{15} SMAs

respective samples support the occurrence of Ti, Ni, and Cu in all the aged samples with a significant intensification of the Cu peak intensity as the nominal copper content increases. The strengthening of Cu peaks in the higher copper alloys is relative, and the intensities of Ni and Ti are also varying, which shows the localized copper enrichment. This is indicative of the idea that aging enhances copper redistribution and segregation especially in cases where the copper concentration in the B_2 TiNi matrix is beyond the solubility level of copper. Combining these SEM and EDX data, it is observed that diffusion-controlled processes increase with the aging, and eventually leads to the growth and coarsening of copper rich secondary components and an increment in porosity of the Cu_{12} and Cu_{15} alloys. This type of microstructural development is consistent with observed behavior of Ti-Ni-Cu SMAs, where aging promotes chemical segregation and stabilization of secondary phases. The current SEM-EDX data provides a solid compositional evidence of copper segregation and secondary phase formation at old condition.

4. Conclusions

Through This study investigated the development and characterization of three Ti-Ni-Cu SMAs $Ti_{50}Ni_{40}Cu_{10}$, $Ti_{50}Ni_{38}Cu_{12}$, and $Ti_{50}Ni_{35}Cu_{15}$, synthesized via powder metallurgy. The effects of various heat treatments, including solution treatment, annealing, and aging, on the SMAs microstructure and properties were explored.

• The results demonstrated that transformation temperatures, as measured by DSC, increase with higher Cu content across all heat treatments.

• The percentage porosity and pore size increase with higher Cu content in all heat treatment processes, although the lowest porosity and smallest pore sizes are found in the annealed samples. SEM/EDX confirmed the presence and size of porosity.

• The optical microscopy showed an increase in grain size with higher Cu content. These results highlight the complex interplay between Cu content, heat treatment processes, and the resulting properties of TiNiCu SMAs, providing valuable insights for optimizing their performance in practical applications.

References

1. Bogue, R. (2009). Shape-memory materials: a review of technology and applications. Assembly Automation, 29(3), 214-219. https://doi.org/10.1108/01445150910972895
2. Parvizi, S., Hashemi, S.M., Asgarinia, F., Nematollahi, M., Elahinia, M. (2021). Effective parameters on the final properties of NiTi-based alloys manufactured by powder metallurgy methods: a review. Progress in Materials Science, 117, 100739. https://doi.org/10.1016/j.pmatsci.2020.100739
3. Ahmad, S., Hashmi, A.W., Singh, J., Arora, K., Tian, Y., Iqbal, F., Al-Dossari, M., Khan, M.I. (2024). Innovations in additive manufacturing of shape memory alloys: alloys, microstructures, treatments, applications. Journal of Materials Research and Technology, 32, 4136-4197. https://doi.org/10.1016/j.jmrt.2024.08.213
4. Singh, R., Singh, R.P., Trehan, R. (2021). State of the art in processing of shape memory alloys with electrical discharge machining: a review. Proceedings of the Institution of Mechanical Engineers, Part B: Journal of Engineering Manufacture, 235(3), 333-366. https://doi.org/10.1177/0954405420958771
5. Aghamiri, S.M.S., Ahmadabadi, M.N., Shahmir, H., Naghdi, F., Raygan, S. (2013a). Study of thermo-mechanical treatment on mechanical-induced phase transformation of NiTi and TiNiCu wires. Journal of the Mechanical Behavior of Biomedical Materials, 21, 32-36. https://doi.org/10.1016/j.jmbbm.2013.01.014
6. Shiva, S., Palani, I.A., Paul, C.P., Mishra, S.K., Singh, B. (2016). Investigations on phase transformation and mechanical characteristics of laser additive manufactured TiNiCu shape memory alloy structures. Journal of Materials Processing Technology, 238, 142-151. https://doi.org/10.1016/j.jmatprotec.2016.07.012
7. Tong, Y., Shuitcev, A., Zheng, Y. (2020). Recent development of TiNi-based shape memory alloys with high cycle stability and high transformation temperature. Advanced Engineering Materials, 22(4), 1900496. https://doi.org/10.1002/adem.201900496
8. Radhamani, R., Balakrishnan, M. (2023). The effect of copper on phase transformation, microstructure and mechanical characterization of Ni50−xTi50Cux shape-memory alloy. Proceedings of the Institution of Mechanical Engineers, Part L: Journal of Materials: Design and Applications, 237(5), 1137-1145. https://doi.org/10.1177/14644207221137257
9. Li, S. (2017). Development and processing of Ti-Ni-based shape memory alloys using laser melting techniques. Ph.D. Dissertation, University of Birmingham, Birmingham, UK.
10. Shiva, S., Yadaiah, N., Palani, I.A., Paul, C.P., Bindra, K.S. (2019). Thermomechanical analyses and characterizations of TiNiCu shape memory alloy structures developed by laser additive manufacturing. Journal of Manufacturing Processes, 48, 98-109. https://doi.org/10.1016/j.jmapro.2019.11.003
11. Lu, H.Z., Liu, L.H., Yang, C., Luo, X., Song, C.H., Wang, Z., Wang, J., Su, Y.D., Ding, Y.F., Zhang, L.C. (2022). Simultaneous enhancement of mechanical and shape memory properties by heat-treatment homogenization of Ti2Ni precipitates in TiNi shape memory alloy fabricated by selective laser melting. Journal of Materials Science & Technology, 101, 205-216. https://doi.org/10.1016/j.jmst.

2021.06.019
12. Zaefferer, S., Ohlert, J., Bleck, W. (2004). A study of microstructure, transformation mechanisms and correlation between microstructure and mechanical properties of a low alloyed TRIP steel. Acta Materialia, 52(9), 2765-2778. https://doi.org/10.1016/j.actamat.2004.02.044
13. Karimzadeh, M., Aboutalebi, M.R., Salehi, M.T., Abbasi, S.M., Morakabati, M. (2015). Effects of thermomechanical treatments on the martensitic transformation and critical stress of Ti-50.2 at.% Ni alloy. Journal of Alloys and Compounds, 637, 171-177. https://doi.org/10.1016/j.jallcom.2015.02.195
14. Panton, B. (2016). Laser processing, thermomechanical processing, and thermomechanical fatigue of NiTi shape memory alloys. Ph.D. Dissertation, University of Waterloo, Waterloo, Canada.
15. Purohit, R., Patel, K.K., Gupta, G.K., Rana, R.S. (2017). Development of Ni-Ti shape memory alloys through novel powder metallurgy route and effect of rolling on their properties. Materials Today: Proceedings, 4(4), 5330-5335. https://doi.org/10.1016/j.matpr.2017.05.043